

# Early LHC Phenomenology of Yukawa-bound Heavy $Q\bar{Q}$ Mesons

Tsedenbaljir Enkhbat<sup>a</sup>, Wei-Shu Hou<sup>a,b</sup>, and Hiroshi Yokoya<sup>a,b</sup>

<sup>a</sup>*Department of Physics, National Taiwan University, Taipei, Taiwan 10617*

<sup>b</sup>*National Center for Theoretical Sciences, National Taiwan University, Taipei, Taiwan 10617*

Current limits from the LHC on fourth generation quarks are already at the unitarity bound of 500 GeV or so. If they exist, the strong Yukawa couplings are turning nonperturbative, and may form bound states. We study the domain of  $m_{b'}$  and  $m_{t'}$  in the range of 500 to 700 GeV, where we expect binding energies are mainly of Yukawa origin, with QCD subdominant. To be consistent with electroweak precision tests, the  $t'$  and  $b'$  quarks have to be nearly degenerate, exhibiting a new “isospin”. Comparing relativistic expansion with a relativistic bound state approach, we find the most interesting is the production of a color octet, isosinglet vector meson (a “gluon-prime”) via  $q\bar{q} \rightarrow \omega_8$ . Leading decay modes are  $\pi_8^\pm W^\mp$ ,  $\pi_8^0 Z^0$ , and constituent quark decay, with  $q\bar{q}$  and  $t't'$  and  $b'b'$  subdominant. The color octet, isovector pseudoscalar  $\pi_8$  meson decays via constituent quark decay, or to  $Wg$ . These decay rates are parameterized by the decay constant, the binding energy and mass differences, and  $V_{tb'}$ . For small  $V_{t'b}$ , one could have a spectacular signal of  $WWg$ , where a soft  $W$  accompanies a very massive  $Wg$  pair. In general, however, one has high multiplicity signals with  $b$ ,  $W$  and  $t$  jet substructures that are not so different from  $t't'$  and  $b'b'$  search.

**PACS numbers:** 14.65.Jk 11.10.St 13.85.Rm 13.25.Jx

## I. INTRODUCTION

The CMS experiment at the Large Hadron Collider (LHC) announced [1] recently that, for Standard Model (SM) with four quark generations (4G), “the Higgs boson in the mass range of 120 to 600 GeV is excluded at the 95% C.L.”. The ATLAS experiment is in agreement [2]. A common inference is that the 4G itself is practically ruled out. Afterall, CMS also reported the most stringent bounds on the  $t'$  and  $b'$  quarks to date:  $m_{t'} > 450$  GeV [1] and  $m_{b'} > 495$  GeV [3], both at 95% C.L., which are rather close to the unitarity bound (UB) of 500–550 GeV [4]. However, in as much as 4G may not exist, an intriguing possibility [5–7] is that electroweak symmetry breaking (EWSB) itself might be triggered by, or related to, the strong Yukawa couplings of the  $t'$  and  $b'$  quarks. Can the UB violation of strong  $WW$  scattering [8] be related to the UB violation of strong  $Q\bar{Q}$  and  $QQ$  scattering? To pursue such questions is a major purpose of the LHC, and is well within its abilities.

If a relatively light Higgs particle emerges soon at the LHC with SM cross sections, then 4G would truly be in trouble [9]. But, the exclusion statement of SM/4G Higgs might well get extended to the SM Higgs itself with 2011-2012 LHC data. For Higgs particle beyond 600 GeV or so, one enters the strong  $WW$  scattering domain, and the “Higgs” becomes a broad object [8, 10], which requires both high energy (14 TeV) and high luminosity to explore. For such a heavy Higgs boson, if the  $t'$  or  $b'$  quarks were however found below 500–550 GeV or so, then the Yukawa sector may not be strongly coupled enough to link with the strongly coupled “Higgs sector”. Thus, we have in mind the scenario where neither the (SM-like) Higgs boson, nor the 4G quarks, are found below 600 GeV and 500–550 GeV, respectively.

It is important to remember that new  $CP$  violating phases associated with 4G quarks may link to [11] the Baryon Asymmetry of the Universe (BAU). Thus, the

existence of a very heavy 4G may touch both EWSB and BAU, which are two of the greatest problems in particle physics. This provides strong motivation for continuing the pursuit of 4G in this volatile time.

If the Higgs boson is heavy (and “fat”), while the 4G quarks are above the UB, then whether the large Yukawa coupling induces  $Q\bar{Q}$  condensation [7] or not, it would be important to explore possible *bound states* of this strong coupling. This is not just about potentially interesting LHC phenomenology, but may be necessary to provide a guide for the search of ultraheavy chiral quarks beyond UB. The main purpose of this paper is to explore lower lying bound states of strong Yukawa coupling, and the associated properties. However, by venturing above the UB, one immediately encounters the perils of the breaking down of perturbation theory. Thus, in lieu of genuine nonperturbative approaches, such as [12] lattice field theory (LFT), our work is only of an illustrative kind.

One aid to the study is a new, heavy isospin. If 4G quarks exist, by which we mean a sequential left-handed doublet and a pair of right-handed singlets under the weak interaction, the  $S$ ,  $T$  variables [13] or electroweak precision tests (EWPrT) require the  $t'$  and  $b'$  to be nearly degenerate (and here, independently, a heavier Higgs is also required [14]). Of course, some small splitting is needed to satisfy  $T$ , but in this paper we will treat the  $t'$  and  $b'$  as degenerate, hence one has a new “isospin”. This isospin, in contrast to the chiral limit of  $u$  and  $d$  quarks under QCD, is in the opposite limit of degenerate *ultra-heavy* quarks. We thus borrow the notation of isovector  $\pi$ ,  $\rho$  (or  $[\bar{t}'b'$ ,  $(\bar{t}'t' - \bar{b}'b')/\sqrt{2}$ ,  $\bar{b}'t'$ ]) and isoscalar  $\eta$ ,  $\omega$  (or  $(\bar{t}'t' + \bar{b}'b')/\sqrt{2}$ ) etc., for the heavy  $Q\bar{Q}$  “mesons”. As we will see, unlike technicolor, the “ $\rho$ ” meson does not play a major role for Yukawa bound states, nor does the  $\eta$ . Another interesting point is that, if the Yukawa interaction is the dominant binding mechanism, since it is color blind, the  $Q\bar{Q}$  mesons, unlike the QCD situation, come not only in color singlets, but color octets as

well [15]. We find the states  $\omega_8$ ,  $\omega_1$ ,  $\pi_8$  and  $\pi_1$ , where the subscript indicates the color representation, to be of phenomenological interest. In particular,  $\omega_8$  and  $\pi_8$  may be accessible in the near future.

In Sec. II, we bring forth the issues of strongly coupled relativistic bound states. We contrast the necessarily relativistic  $\gamma_5$  coupling of weak Nambu–Goldstone boson (NG), or longitudinal vector boson exchange, to the Coulombic QCD bound state, as well as scalar exchange. Because the Higgs scalar should be treated as heavy now, its effect is less prominent than NG exchange. We compare the traditional relativistic expansion [15] with a relativistic Bethe-Salpeter approach [16], and illustrate why the Yukawa bound state involves highly relativistic motion of its constituents. An issue appears regarding the treatment of  $s$ -channel NG exchange, towards strong Yukawa binding. This, plus other issues, forces us to compromise in the study of the possible spectrum at this stage, and we restrict ourselves to  $m_Q$  in the range of 500–700 GeV, i.e. not far above the UB. In this way, the relativistic expansion provides a partial guide, while we offer a peek beyond and consider binding energies of order  $-100$  GeV or more, for the possible spectrum around and above the TeV scale. This leads us to focus on, from the production point of view, an  $\omega_8$  state (effectively a “ $g$ ”, or gluon-prime), as well as possibly the  $\pi_8$  and  $\omega_1$  states in its decay final state.

In Sec. III we turn to exploring the production and decay properties. We survey the key parameters needed: the binding energy, the vector–pseudoscalar and octet–singlet mass splittings, the vector meson decay constant  $f_{\omega_8}$ , and the quark mixing element  $V_{tb}$ . Production is mostly through  $q\bar{q} \rightarrow \omega_8$  and depend only on  $f_{\omega_8}$ , but the annihilation, transition, and free quark decays involve all these parameters, where the numerical values we use are only illustrative. We find, in general, that the  $\omega_8$  is relatively narrow, but has a host of decay final states, which might therefore elude early detection. We offer some discussion of the phenomenology at LHC in Sec. IV, touching briefly on *deep* bound states, i.e. the possibility of binding energy approaching  $m_Q$  itself, for  $m_Q$  beyond 700 GeV. We end with a conclusion and outlook.

## II. STRONGLY COUPLED RELATIVISTIC BOUND STATES

When the unitarity bound is reached for very heavy chiral quarks, it means that some *tree level*  $Q\bar{Q}$  and  $QQ$  scattering cross sections will violate unitarity, or conservation of probability, in the high energy limit. Pointed out over 30 years ago [4], it is remarkable that we are now at the doorsteps to probe whether such new heavy chiral quarks exist.

Many, if not most people, tacitly take the UB as a kind of ceiling for SM-like chiral quarks to make sense. But in reality, crossing the UB just implies that the Yukawa couplings are becoming so strong, they are turning non-

perturbative. We have seen how the remarkable theory of QCD turns nonperturbative in the infrared, resulting in the rich phenomena of hadrons. We will not dwell on deeper short-distance (UV) gauge theories like technicolor, but just take the large Yukawa couplings [17] at face value: if chiral quarks  $Q$  (a left-handed doublet of  $t'$  and  $b'$  in our case) exist at or above the UB, what could be the emergent phenomena?

Consider first heavy quarkonia bound by QCD. Since QCD is perturbative at short distance, we have the familiar Coulombic bound states with a  $1/\beta$  enhancement factor, where  $\beta = v$  is the velocity. This is the domain of Non-Relativistic QCD (NRQCD), where one expands in velocity, which is of order  $\alpha_S$ . The NR nature makes good contact with the familiar atomic systems.

Exchanging Higgs bosons brings in the Yukawa couplings, which has been considered in the literature. For our case, we will treat the Higgs boson as above [1, 2] 600 GeV and heavy, which suppresses the binding effect due to Higgs exchange. However, NG or longitudinal vector boson exchange (transverse gauge boson exchange has coupling constant  $g$  or  $e$ , hence subdominant and largely ignored by us) also couples with the Yukawa coupling strength, but it involves the  $\gamma_5$ , which couples the upper and lower components of the massive Dirac quark. Since the lower component vanishes when the heavy quark is at rest, NG exchange is suppressed in the NR limit. Conversely, the coupling to high momentum heavy quarks is large, the more so the heavier the quark. This reflects the derivative coupling nature of longitudinal vector bosons. The upshot is that, Yukawa interactions between very heavy quarks are large when these quarks are in relativistic relative motion, i.e. with momentum  $q \sim m_Q$ .

With this insight, and ignoring the Higgs exchange for the moment, if the bound state formation is dominated by QCD, then the NR nature of the bound state ( $\beta \simeq \alpha_S$ ) actually suppresses the effect of Yukawa coupling. However, as the Yukawa coupling increases with  $m_Q$ , although the QCD-bound system becomes even more non-relativistic, at some point NG exchange would (perhaps suddenly) take over, and one would find the bound state system turns ultrarelativistic.

We shall illustrate with two different perspectives, one a traditional relativistic expansion [15], the other a relativistic Bethe-Salpeter approach [16].

### A. Relativistic Expansion

A standard approach in considering bound state phenomena is to make a relativistic expansion around the leading potential. The Higgs potential for very heavy quarks, in the context of forming bound states, was considered a long time ago [18]. The relativistic corrections were recently calculated in Ref. [15]. The scattering amplitudes for  $t$ -channel Higgs, neutral and charged NG (called fictitious scalar in Ref. [15]), and gluon exchange, as well as  $s$ -channel NG exchange, were com-

puted. Ref. [15], however, did not put in  $s$ -channel Higgs and gluon exchange, even though both color singlet and octet  $Q\bar{Q}$  configurations were discussed. Touching both  $m_H = 130$  GeV and  $m_H = m_Q$  cases, a variational approach was used to estimate the size  $a_0$  (equivalent to wavefunction) and binding energy for  $I = 0, 1, S = 0, 1$ , color singlet and octet states.

We will not repeat what was already done here, but just give some salient features. As a control on validity of the relativistic ( $v$  or  $\beta$ ) expansion, the authors of Ref. [15] required  $\mathbf{q}^2/m_Q^2 < 1/3$  ( $|\mathbf{q}| \equiv q$  is the relative momentum), which translates into  $a_0 > \sqrt{3}/m_Q$ . Since  $t$ -channel gluon exchange gives the Coulomb potential, it is clear that one has a Coulombic QCD bound state when  $m_Q$  is not yet too large, with Bohr radius  $a_{\text{QCD}}$ .

The low mass Higgs case is no longer tenable with 4G, both by direct search [1, 2], and indirectly [14] from EW-PrT due to the heaviness of 4G quarks. For the heavy Higgs case illustrated with  $m_H = m_Q$ , as one can see from Fig. 8 of Ref. [15], the radii  $a_0$  of the  $\omega_1$ ,  $\rho_1$  and  $\eta_1$  (the subscript 1 stands for color singlet) states decrease rather slowly below  $a_{\text{QCD}}$  as  $m_Q$  increases. The  $\pi_1$  radius rises slowly above  $a_{\text{QCD}}$  due to the extra repulsion it receives from  $s$ -channel NG exchange. The Yukawa effect is subdominant compared with QCD, where inspection of the binding energies offer further support: they rise slowly from  $\sim -1$  GeV around  $m_Q = 200$  GeV, to  $\sim -2$  GeV at  $m_Q = 300$  GeV, with  $\pi_1$  only slightly lower. However, just before  $m_Q$  reaches 400 GeV, radius  $a_0$  for  $\omega_1$  drops precipitously, while the binding energy rises sharply from around  $-2.5$  GeV, to around  $-100$  GeV at  $m_Q = 500$  GeV. The condition  $a_0 > \sqrt{3}/m_Q$  is violated shortly above  $m_Q = 400$  GeV.

The ‘‘kink’’ around 400 GeV is the point where the NG exchange has wrestled the mechanism for binding away from the usual NR QCD binding. The sudden drop of the size of the bound state is due to tapping the large attraction at large momentum  $q$  for the bound quark (besides the  $\gamma_5$  coupling of the NG bosons, the heavy Higgs also defines a very short range for the strong Yukawa coupling to be effective). The resulting larger binding energy overcomes the much increased kinetic energy. For  $\rho_1$ , the onset is delayed until  $m_Q = 530$  GeV or so, with binding energy of  $-25$  GeV at  $m_Q = 600$  GeV.

For color octet states, which are not bound by QCD, the binding energy for  $\omega_8$ , due purely to Yukawa coupling, turns on sharply around  $m_Q = 535$  GeV, rising to  $-35$  GeV for  $m_Q = 600$  GeV. The  $\rho_8$  state turns on much later, around  $m_Q = 700$  GeV. But, unlike  $\pi_1$ , because there is no  $s$ -channel repulsion,  $\pi_8$  is degenerate with  $\omega_8$ . It should be noted that the Yukawa effects of neutral and charged NG exchange is weaker but constructive for  $\omega_8$ , while the converse is true for  $\pi_8$ , so this degeneracy could be accidental. Furthermore, this degeneracy should be lifted by  $s$ -channel gluon annihilation, which would raise  $m_{\omega_8}$  but was not considered by the authors of Ref. [15]. As we shall soon see, the vector channel also has  $S$ - and  $D$ -wave mixing.

Although identifying the  $\omega_1$  as the lightest color singlet, and  $\omega_8$  (and  $\pi_8$ ) as the lightest color octet, it is ironic that the relativistic expansion breaks down almost immediately after the strong Yukawa binding becomes potent. But it does illustrate that one needs a genuine relativistic approach in treating strong Yukawa binding. We turn to such an approach that is in principle non-perturbative, but carrying its own dubious features: the Bethe-Salpeter (BS) equation.

## B. Relativistic Bethe-Salpeter Approach

A long time ago, around the time the SSC (Superconducting Super Collider) was under construction but then unfortunately canceled, the authors of Ref. [16] pursued the BS equation approach to the relativistic bound states of very heavy sequential 4th generation quarks. It consists of a ladder sum of the scattering amplitudes that appear in the relativistic expansion. In the heavy isospin limit and treating  $M_Z = M_W$ , a clear isospin reorganization separates into  $I = 0$  and  $I = 1$  ‘‘mesons’’.

For  $Q\bar{Q}$  meson with total momentum  $P$  and relative momentum  $q$ , one has a set of integral equations, with loop momentum  $q'$ , where  $q' - q$  is the momentum exchange in  $t$ -channel. However, for  $s$ -channel annihilation contribution, the annihilation momentum is  $P$  itself, and the integral over loop momentum  $q'$  carries no  $q$  dependence, giving a possibly divergent constant. To remedy this, Ref. [16] took a fixed  $q$  subtraction at  $q = 0$ . In this way, all the  $s$ -channel diagram contributions were eliminated from the BS equation. This includes even the  $s$ -channel gluon exchange for the octet, isosinglet vector channel, which was not considered in Ref. [16], as the authors concerned themselves with color singlet states only.

In terms of mathematical physics, to set up integral equations to be solved in a self-consistent way, the subtraction at constant  $q$  seems reasonable. However, as admitted by the authors of Ref. [16] in a footnote, the  $s$ -channel NG exchange leads to repulsion. Thus, in discussing bound state solutions, there is the issue of the physical correspondence, and therefore the range of validity (in  $m_Q$ ) for implementing the subtraction. In the relativistic expansion, one clearly would not drop the  $s$ -channel diagrams.

Our purpose here is not to make a full treatment of the BS equation, as it is only a ladder sum of  $t$ -channel exchange diagrams, with higher order corrections ignored. Furthermore, while the BS equation is relativistic, its solution depends very much on the approximations and ansatz made. Ref. [16] illustrated with covariant gauge (but employing a weak coupling relation between spatial and temporal spinor components), the instantaneous approximation with positive frequency potential only, as well as keeping both positive and negative frequency potentials. Although the numerical solutions share common features, the bound state mass ( $M$ ) values differ. Starting all from  $M \cong 2m_Q$  for low  $m_Q$ , they decrease

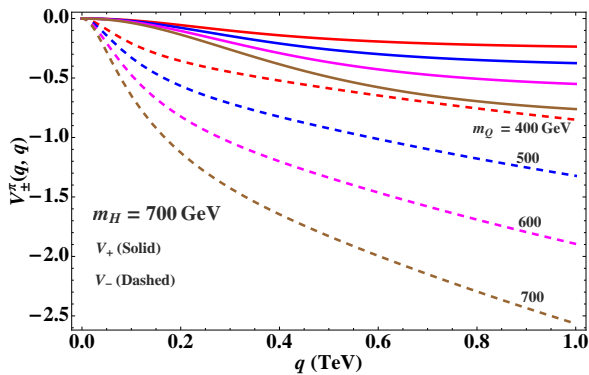


FIG. 1. The  $V_+^\pi$  (solid) and  $V_-^\pi$  (dashed) potentials in Eq. (1) for the  $\pi_1$  state, for  $m_Q = 400, 500, 600, 700$  GeV, and  $m_H = 700$  GeV, plotted along  $q' = q$ . Both vanish for  $q = 0$ , or zero relative motion, but go to rather large values for large  $q$ , with  $V_-^\pi$  turning on rather sharply for  $q \gtrsim 100$  GeV.

smoothly as  $m_Q$  increases, without exhibiting the kink seen in the relativistic expansion. As such, the BS approach is an improvement. But, as a common feature, once the binding energy  $M - 2m_Q$  becomes significant (e.g.  $-100$  GeV or so), at high enough  $m_Q$ , the low lying mesons collapse. That is, the binding energy becomes so large such that the total mass drops to zero.

Having bound state solutions numerically turning tachyonic for a strongly coupled system is not particularly astounding. For QCD (and likewise for QED), quarkonium masses calculated at fixed order could also vanish at large enough coupling strength. The system has turned fully relativistic with strong coupling, and the familiar Bohr-Schrödinger solution is no longer valid. For the BS equation, however, it is already relativistic. The collapse of the meson state may be related to the symmetry breaking itself [21], but because of the approximate nature of the BS equation, as well as the numerical approximations made in its solution, we refrain from dwelling further on this.

Rather, we wish to use the BS equation and its numerical study to compare and contrast with the previously discussed relativistic expansion, to project what may really happen for relativistic, strong Yukawa bound states, before any “collapse”, such as illustrated in Ref. [16], could occur. For this purpose, we note that with the *subtracted* BS equation, hence with the *s*-channel repulsion removed, the  $\pi_1$  turns out to be the most attractive system, i.e. the lightest bound state: the NG, gluon and Higgs exchange are all attractive, as can be seen also from Ref. [15]. The behavior for  $\omega_1$  is indeed similar, but the formalism is more complicated for the  $1^-$  system, where the *S*- and *D*-wave channels are coupled. Note that Ref. [16] used (sometimes tacitly) a Higgs mass around 100 GeV, which is no longer valid. In our mind, we are interested in the bound state dominated by Yukawa coupling, i.e. by NG exchange, hence we will view gluonic exchange as correction, with Higgs exchange perhaps even

milder. This matches to what one finds in the relativistic expansion, that the Yukawa binding suddenly turns on, bringing on a rapid rise in binding energy. In effect, we use the BS equation approach to check, and probe beyond, the “kink” seen in the relativistic expansion.

The equation for  $\pi_1$  is the most compact. In the impulse approximation, integrating over  $q_0$  gives the amplitude  $\chi(q)$ , where  $q = |\mathbf{q}|$  is the relative momentum. Keeping both positive and negative frequency amplitudes  $\chi_\pm(q)$ , one has the coupled equations,

$$(M \mp 2\omega)\chi_\pm^\pi(q) = \pm \int dq' \frac{q'}{q} [V_\pm^\pi(q, q')\chi_\pm^\pi(q') + V_\mp^\pi(q, q')\chi_\mp^\pi(q')], \quad (1)$$

where  $M$  is the eigenvalue, and  $\omega = \sqrt{m^2 + q^2}$ . The potentials  $V_\pm^\pi(q, q')$ , where we have absorbed a factor of  $1/\pi$  into its definition as compared to Ref. [16], arise from *t*-channel diagrams as described earlier.

Let us understand the  $V_+$  and  $V_-$  potentials. The less familiar one is  $V_-$ , which couples  $\chi_\mp$  to  $\chi_\pm$ , while  $V_+$  is “diagonal”. In the limit that  $|V_+| \gg |V_-|$ , one simply has  $M = 2\omega + \langle V_+ \rangle$ , where  $\langle V_+ \rangle$  is analogous to the expectation value of the potential ( $\chi_+(q)$  is like  $\psi^\dagger\psi$ ) of nonrelativistic quantum mechanics. On the other hand, if  $2\omega \gg |V_-| \gg |V_+|$ , then  $M \simeq 2\omega - V_-^2/4\omega$ , hence the  $V_-$  contribution is more suppressed than the corresponding  $V_+$  contribution when it is weak.

The potentials  $V_\pm(q, q')$  are symmetric in  $q$  and  $q'$ , and is steepest along  $q' = q$ . We plot  $V_\pm^\pi(q, q)$  in Fig. 1, for heavy  $m_H = 700$  GeV, and for  $m_Q = 400, 500, 600, 700$  GeV. We have checked that the  $V_+^\pi$  potential drops by a factor of two or more as  $m_H$  moves from 100 to 700 GeV, but  $V_-^\pi$  is rather insensitive to  $m_H$ . We see from Fig. 1 that both the  $V_+^\pi$  and  $V_-^\pi$  potentials are suppressed for low relative momentum  $q$ , agreeing with the relativistic expansion view. As  $q$  increases,  $V_+^\pi$  increases relatively slowly, reaching  $-V_+^\pi \simeq 0.3$  (0.7) at  $q = 500$  (700) GeV for  $m_Q = 500$  (700) GeV. But  $V_-^\pi$  turns on more sharply, reaching beyond  $-V_-^\pi \simeq 1$  at  $q = m_Q = 500$  GeV, and  $-V_-^\pi \simeq 2$  at  $q = m_Q = 700$  GeV.

So what does the strength of  $V_\mp^\pi$  mean? Take the  $\chi_+^\pi$  equation, the binding energy  $E = M - 2m_Q$  is equal to  $2\omega - 2m_Q$ , the kinetic energy due to motion, plus the right hand side of Eq. (1), which should be the “potential”. Let us normalize  $q'$  by  $m_Q$ . Since  $V_\pm^\pi(q, q')$  is steepest for  $q' = q$ , we see that  $m_Q|V_\mp^\pi(q, q)| \simeq m_Q$  for  $q \simeq m_Q$  means the “potential” is comparable to  $m_Q$  in strength when the momentum is comparable to the rest mass, and the kinetic energy due to motion is  $2(\sqrt{2} - 1)m_Q$ . We can now sense why there is a tendency for the  $\pi_1$  state to collapse already for  $m_Q$  not far above 500 GeV in the numerics of Ref. [16].

### C. Possible Spectrum for $m_Q \simeq 500$ –700 GeV

We have illustrated how the binding energy for the (heavy) isovector, color singlet  $0^-$  state, which we call

$\pi_1$ , could be already moving towards collapse for  $m_Q$  as low as 500 GeV (this number from Ref. [16] contains the attraction due to light Higgs exchange), if the BS approach of Eq. (1) holds true. However, this state receives a repulsive  $s$ -channel NG annihilation contribution. Furthermore, as the tendency towards collapse approaches, the ladder sum BS equation may no longer be sufficient. Even within the BS approach, where Eq. (1) gives rise to the earliest collapse, if one drops the negative frequency amplitude, the collapse is delayed [16] by almost a factor of two in  $m_Q$ . In the covariant gauge but using a weak coupling relation between temporal and spatial spinor components, the collapse of  $\pi_1$  occurs slightly before the positive frequency only case. It is not clear at what  $m_Q$  the collapse truly occurs numerically. In any case, we would not touch the collapse here, as it is not yet well understood. It seems prudent, then, to consider binding energies of  $-100$  to  $-200$  GeV, but not more, to make a preliminary study of possible phenomena at LHC, running at  $\sqrt{s} = 7$  TeV.

A similar equation as Eq. (1) holds for the isosinglet, color singlet  $0^-$  state, the  $\eta_1$ . Although gluon and Higgs exchange are attractive, NG exchange turns repulsive [15, 16]. Thus,  $\eta_1$  is much heavier than  $\pi_1$ , and cannot be a low-lying state.

Turning to vector mesons, Ref. [16] found, similar to the relativistic expansion of Ref. [15], that the isoscalar  $\omega_1$  has the tightest binding, though it is weaker than ( $s$ -channel subtracted)  $\pi_1$ . This concurs with our earlier observation that Yukawa effects are weaker but constructive for vector, while stronger but destructive for pseudoscalar. However, there is no repulsive  $s$ -channel effect for  $\omega_1$ . On the other hand, checking the formalism, we find that there is  ${}^3S_1$ - ${}^3D_1$  mixing, resulting in a set of more complicated coupled BS equations. From the numerics of Ref. [16], we expect that for  $m_Q$  in the range of 500–700 GeV, binding energies of order  $-100$  to  $-200$  GeV is reasonable for  $\omega_1$ . The  $\rho_1$  state, analogous to  $\eta_1$  in receiving the repulsive NG exchange, is far less binding, which is also seen from the relativistic expansion.

Turning to color octet counterparts, one can treat gluon exchange as a perturbation when binding energies are much large than QCD bound states. Given that the bound state should be rather small, the repulsion due to gluon exchange should be larger than typical QCD binding. But without fully solving for the bound state, octet-singlet splitting is uncertain. However, there should be no doubt that  $\pi_8$  and  $\omega_8$  would be the low-lying octet states, in agreement with the relativistic expansion. The octet  $\eta_8$  and  $\rho_8$  are likely not (or at best weakly) bound, hence we do not consider these.

To summarize, the states to keep in mind are  $\pi_1$ ,  $\omega_1$ ,  $\pi_8$  and  $\omega_8$ . There are possibly other states with different quantum numbers, but in general they would not be lighter, while likely possessing more complicated properties. The absence of  $\rho$  states is distinct from QCD-like gauge theories such as technicolor. For  $m_Q$  in the range of 500 to 700 GeV, staying short of very tight bind-

ing, these states would probably populate the 1 to 1.4 TeV range, with binding energies of order  $-100$  to  $-200$  GeV. The ordering of the spectra, according to Ref. [16] (which did not actually consider octet states), would be  $M_{\pi_1} \lesssim M_{\omega_1} \lesssim M_{\pi_8} \lesssim M_{\omega_8}$ .

Since we are concerned with LHC phenomenology and the heavy quark search program in the near future, we should consider briefly issues regarding production:

- $\pi_1$  and  $\omega_1$  cannot be produced via  $gg$  fusion, but can be produced via weak Drell-Yan processes, hence have a weak production cross section;
- $\pi_8$  can be pair produced by  $gg$  and  $q\bar{q}$  scattering [19], but it is heavier and less efficient at 7 TeV.

This leaves  $\omega_8$ , which has the same quantum numbers as the gluon, that is the most attractive in the near future in terms of production cross section. It cannot be produced by  $gg$  fusion, as two massless vectors cannot forge a massive vector (Yang's theorem) particle, hence the production is limited to  $q\bar{q}$  fusion. In the next section, we turn to the production and decay properties of the  $\omega_8$  meson. Note that if an  $\eta_8$  or  $\eta_1$  state existed, such as for QCD binding, it could tap  $gg$  production [20].

### III. PRODUCTION AND DECAY OF $\omega_8$

In this section, we discuss the production and decay of the  $\omega_8$  meson, which we have portrayed as the likely leading harbinger of 4G bound-states in our scenario, where a very heavy quark *isospin* symmetry prevents the production of some mesons directly at hadron colliders.

For the numerical study of the production cross-sections and decay rates, the following parameters are needed as input: the decay constant  $f_{\omega_8}$ , the 4G quark masses  $m_Q = m_{t'} = m_{b'}$  (we assume degeneracy of  $t'$  and  $b'$  as a simplifying approximation, hence an isospin symmetry), the mass of resonances, *i.e.* the binding energy of resonances, and finally the quark mixing elements  $|V_{t'b}| \cong |V_{tb'}|$ . Once the constituents as well as their interactions are fixed, the decay constant and binding energy are the consequence of the dynamics of the system. As we stressed previously, in the range of strong Yukawa couplings we consider, their estimation has to be done by LFT approach [12] for more quantitative understanding. However, such an endeavor is beyond the scope of this paper. Instead we parameterize them in our phenomenological study.

The decay constant of  $\omega_8$  is defined through

$$\langle 0|V^{\mu,a}|\omega_8^b(p)\rangle \equiv \frac{1}{\sqrt{2}}\delta^{ab}f_{\omega_8}m_{\omega_8}\varepsilon^\mu(p), \quad (2)$$

which we parameterize by a dimensionless parameter  $\xi = f_{\omega_8}/m_{\omega_8}$ . The mass  $m_{\omega_8}$  is the most important, as we discuss the production and decay of  $\omega_8$ . We also assume  $|V_{t'b}| = |V_{tb'}|$  is the dominant quark mixing element, and ignore mixings with lighter generations.

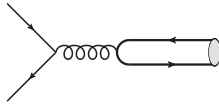


FIG. 2. Production mechanism for the color octet, isoscalar-vector meson  $\omega_8$  at hadron colliders.

### A. Production

The dominant production mechanism for  $\omega_8$  is, as illustrated in Fig. 2, via  $q\bar{q}$  annihilation. Because one cannot fuse two massless gluons into a massive vector boson, gluon-gluon fusion is not operative. We have also computed the higher order  $gg \rightarrow \omega_8 g$  process as a check.

At the parton level, the total cross section is

$$\hat{\sigma}_{q\bar{q} \rightarrow \omega_8}(\hat{s}) = \frac{32\pi^3 \alpha_s^2}{9m_{\omega_8}^2} \xi^2 \delta(1 - m_{\omega_8}^2/\hat{s}). \quad (3)$$

Convolving with the parton luminosity

$$\mathcal{L}(\tau; \mu_F^2) = \int \int dx_1 dx_2 f_1(x_1; \mu_F^2) f_2(x_2; \mu_F^2) \delta(\tau - x_1 x_2),$$

we get the hadronic cross section,

$$\sigma(s) = \int d\hat{\tau} \hat{\sigma}(\hat{\tau}s) \mathcal{L}(\hat{\tau}; \mu_F^2). \quad (4)$$

We plot on the left-hand side of Fig. 3 the cross section for inclusive  $\omega_8$  production at the LHC with  $\sqrt{s} = 7$  TeV. We use CTEQ6L [22] parton distribution functions (PDFs), and set the renormalization and factorization scales to  $\mu_R = \mu_F = m_{\omega_8}$ . We use three values of  $\xi = f_{\omega_8}/m_{\omega_8} = 0.1, 0.03$  and  $0.01$  for illustration. Although we do not have any suggestive estimation for the decay constant, since the Yukawa bound state is highly relativistic, we expect the larger (smaller) value of  $\xi$  corresponds to a stronger (weaker) bound meson. We note that the decay constant divided by meson mass for usual  $\rho$ ,  $J/\psi$  and  $\Upsilon$  are  $\mathcal{O}(0.1)$ . However, we are not dealing with usual QCD-bound meson production [23, 24], so we leave  $\xi$  as a parameter. The cross section is proportional to  $\xi^2$  and decreases with increasing  $m_{\omega_8}$ . Because of our ignorance of the decay constant  $f_{\omega_8}$ , the cross section  $\sigma_{\omega_8}$  ranges from pb to fb, for  $m_{\omega_8}$  ranging from 900 to 1400 TeV. The plot extends to 2 TeV, since it depends only on  $\xi$ , which we view should be experimentally determined. As the gluon density at the LHC is large, we have checked the higher order  $gg \rightarrow \omega_8 g$  scattering process, and find the contributions to be quite small for the region of our interest,  $m_{\omega_8} > 0.8$  TeV.

For comparison, we also plot the open  $Q\bar{Q}$  pair production cross section at LO and NLO [25], as a function of  $2m_Q$ , matching (approximately) to  $m_{\omega_8} = 2m_Q$  on the same plot. The cross section should be multiplied by two to take into account the production of the degenerate 4G doublet. In NLO calculation, we use CTEQ6M

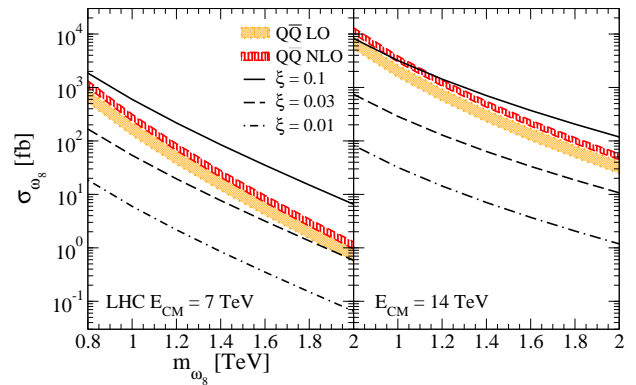


FIG. 3. Production cross-section of  $\omega_8$  at the LHC running at 7 TeV (left) and 14 TeV (right) for various  $\xi = f_{\omega_8}/m_{\omega_8}$  values. The open  $Q\bar{Q}$  cross sections at LO and NLO are also plotted for comparison.

PDFs [22]. To see the uncertainty of the cross section, as well as the size of NLO correction, we vary the scales in each calculation from  $\mu_R = \mu_F = m_Q$  to  $4m_Q$ . The uncertainty for LO (NLO) prediction is expressed as the dotted (hatched) band.

At the LHC running at 7 TeV, the  $\omega_8$  production cross section with  $\xi = 0.1$  is about the same order as twice the open  $Q\bar{Q}$  production cross section in the lower mass region, but exceeds the latter in the higher mass region. On the other hand, when  $\xi$  is smaller, the cross section could be well below the open production cross section. Thus,  $\omega_8$  production can be interesting if  $\xi$  is sizable, such as of 0.1 order. Note that  $\omega_8$  is produced through  $q\bar{q}$ , while open  $Q\bar{Q}$  is produced dominantly through  $gg$  fusion.

We plot on the right-hand side of Fig. 3 the  $\omega_8$  cross section for LHC at  $\sqrt{s} = 14$  TeV, which is an order of magnitude larger than those for LHC at 7 TeV. The open production cross section grows relatively larger than the  $\omega_8$  production because of increase in gluon luminosities.

### B. Decay

The decay channels of  $\omega_8$  we consider are

- Annihilation Decay:  $\omega_8 \rightarrow q\bar{q}, t\bar{t}, t\bar{t}', b\bar{b}'$ ;
- Free-quark Decay:  $\omega_8 \rightarrow bW\bar{t}', tW\bar{b}'$ ;
- Meson Transition:  $\omega_8 \rightarrow \omega_1 g; \pi_8 W$ .

In the following, we discuss each decay mode separately.

#### 1. Annihilation Decay

First,  $\omega_8$  can decay into dijets or  $t\bar{t}$  by the co-annihilation of the 4G quarks inside the bound state

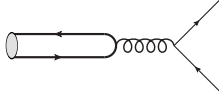


FIG. 4. QCD-induced annihilation decay of  $\omega_8$  into light quark pair (dijets) or  $t\bar{t}$ .



FIG. 5. Weak decay modes: (a) exchange diagram with off-diagonal quark mixing element; (b) free quark decay.

through QCD, as shown in Fig. 4. These are the reverse processes of the production mechanism, therefore the existence of these decay modes is robust.

The decay partial width in this mode is proportional to  $\xi^2$ . The two-body decay width is calculated at Born level to be

$$\Gamma(\omega_8 \rightarrow q\bar{q}) = \xi^2 \frac{\pi\alpha_s^2}{3} m_{\omega_8} n_f, \quad (5)$$

$$\Gamma(\omega_8 \rightarrow t\bar{t}) = \xi^2 \frac{\pi\alpha_s^2}{3} m_{\omega_8} \beta_t, \quad (6)$$

where  $n_f = 5$  is the number of light quark flavors, and  $\beta_t = \sqrt{1 - 4m_t^2/m_{\omega_8}^2}$  is the velocity of the top quark in the  $\omega_8$  rest-frame. Due to the number of light quark flavors, the decay partial width into dijets is larger than that into  $t\bar{t}$  by  $\sim 5$ .

Analogous to  $gg \rightarrow \omega_8 g$  production, we have also estimated the three-body  $\omega_8 \rightarrow ggg$  decay rate, following the tree-level calculation of Ref. [26], and found that it can be ignored.

Another type of annihilation decay channel is caused by weak boson exchange, where an off-diagonal quark mixing element acts on one of the bound quarks, as shown in Fig. 5(a). This is rather similar to the binding mechanism, where the quark mixing elements are always within 4G. Once the cross-generation interaction occurs, the recoil due to the energy release from the mass difference between the 4G quarks and lower generations would eject the lighter quark and destroy the bound state, followed by subsequent decay of the leftover 4G quark. The lower generation quark mass is too light such that it cannot bind with the heavy 4G quark by Yukawa coupling.

The decay width is calculated in terms of the decay constant in Eq. (2) using the Fierz identity for the current products, giving ( $\hat{m} \equiv m/m_{\omega_8}$ )

$$\Gamma(\omega_8 \rightarrow t\bar{t}) = \xi^2 |V_{tb}^* V_{t'b'}|^2 \frac{G_F^2 m_{\omega_8}^5}{192\pi} E(\hat{m}_t, \hat{m}_{t'}), \quad (7)$$

$$\Gamma(\omega_8 \rightarrow b\bar{b}') = \xi^2 |V_{t'b'}^* V_{t'b}|^2 \frac{G_F^2 m_{\omega_8}^5}{192\pi} E(\hat{m}_b, \hat{m}_{b'}), \quad (8)$$

where

$$E(x, x') = \frac{\lambda(1, x^2, x'^2)}{2(1 - 2x^2 - 2x'^2)^2} \times \left[ 2 - 9x^2 + 15x^4 - 8x^6 - 9x'^2 + 18x^2 x'^2 - 8x^4 x'^2 - 16x^6 x'^2 + 15x'^4 - 8x^2 x'^4 + 32x^4 x'^4 - 8x'^6 - 16x^2 x'^6 \right]. \quad (9)$$

with  $\lambda(a, b, c) = \sqrt{a^2 + b^2 + c^2 - 2(ab + bc + ca)}$ . The charge conjugate decays have the same partial width as above. We have actually performed a full calculation, but set  $M_W$ , or weak coupling  $g$ , to zero at the end, as we are concerned with longitudinal vector boson exchange. We have also not distinguished between  $2m_{t'}$  and  $m_{\omega_8}$ , where the latter provides the scale parameter. The decay rate depends on both the off-diagonal quark mixing element  $|V_{t'b}| = |V_{tb'}|$  as well as  $\xi$ .

In this mode,  $\omega_8$  decays into on-shell  $t\bar{t}'$  or  $b\bar{b}'$  (and conjugate). If we restrict to  $t' \rightarrow bW$  and  $b' \rightarrow tW \rightarrow bWW$  for the decay of 4G quarks, the final state all end up as  $bWbW$ . The signal is similar to  $t\bar{t}$  production, but the kinematical distribution differs from the standard model counterpart.

## 2. Free Quark Decay

A second type of decay mode is induced by the decay of the constituent quarks, as illustrated in Fig. 5(b). It is similar to the weak boson exchange decay discussed just before, and quantum mechanically speaking, the exchanged boson escapes the system as an on-shell particle. We call this the “free” quark decay mode, even though the decaying quark is bound. The decay partial width in this mode depends crucially on  $V_{t'b}$  and  $V_{t'b'}$ , but not strongly on the structure of  $\omega_8$ . This last statement would no longer hold when one enters the realm of deeply bound states, where binding energy is much larger than the  $-100$  GeV adopted here.

Inside the bound state system, the decay of the constituents is suppressed by phase-space and time dilatation effects [27, 28]. That is, the decaying quark constituent is off-shell. However, for simplicity, we ignore these effects in our rate calculation, and use

$$\Gamma_{\text{free}} \simeq \frac{1}{2} [2\Gamma_{t'} + 2\Gamma_{b'}] = \Gamma_{t'} + \Gamma_{b'}, \quad (10)$$

where  $\Gamma_{t'}$ ,  $\Gamma_{b'}$  are given at Born level as

$$\Gamma_{t'}(m_{t'}) = |V_{t'b}|^2 \frac{G_F m_{t'}^3}{8\sqrt{2}\pi} F(\tilde{m}_W, \tilde{m}_b), \quad (11)$$

$$\Gamma_{b'}(m_{b'}) = |V_{t'b'}|^2 \frac{G_F m_{b'}^3}{8\sqrt{2}\pi} F(\tilde{m}_W, \tilde{m}_t), \quad (12)$$

with  $\tilde{m} = m/m_{t'}$  or  $m/m_{b'}$ , and

$$F(x, y) = (1 + x^2 - 2x^4 - 2y^2 + x^2 y^2 + y^4) \lambda(1, x^2, y^2) \quad (13)$$

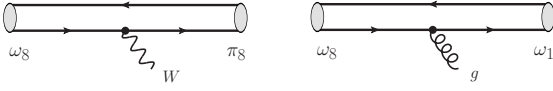


FIG. 6. Meson transition currents for  $\omega_8 \rightarrow \pi_8$ , and  $\omega_8 \rightarrow \omega_1$ .

with  $\lambda(a, b, c)$  as defined earlier. Note that we have kept  $M_W$  here, since the decay process is quite similar to the familiar top quark decay.

The decay width of the 4G quarks is suppressed by the small  $V_{t'b}$  and  $V_{tb'}$ , but grows rapidly with the 4G quark mass. If  $\omega_8$  decays through  $t'$ , the final state would be  $bWbW$ , and  $bWWWbWW$  if decay is through  $b'$ . The search of these signal can be along the standard 4G quark search strategy [29], except that, if heavy quark mass could be reconstructed, then for example one  $bW$  pair has a lower mass (due to binding energy) than the other  $bW$  pair from on-shell  $t'$  decay [30].

### 3. Meson Transition Decay

Finally, a third class of decay is for  $\omega_8$  to turn into other resonances. We consider the two channels of  $\omega_8 \rightarrow \pi_8 W$  and  $\omega_8 \rightarrow \omega_1 g$ . The other possible channel  $\omega_8 \rightarrow \pi_1 g$  is forbidden by the heavy isospin. The partial width for these decays depend on the mass difference as well as the transition amplitude of these resonances. The meson transition to  $\pi_8 W$  would open only if  $m_{\omega_8} - m_{\pi_8} > m_W$ . For  $m_{\omega_8} - m_{\pi_8} < m_W$ ,  $\omega_8$  can decay into  $\pi_8 \ell \nu_\ell$  or  $\pi_8 q \bar{q}'$  through the off-shell  $W$  boson. However, the partial width would be negligibly small.

We can write down a general vector to pseudoscalar transition amplitude via (color singlet) vector or axial-vector currents as,

$$\langle \pi_8^a(p') | V^\mu | \omega_8^b(p) \rangle = \frac{\delta^{ab}}{\sqrt{m_{\pi_8} m_{\omega_8}}} V(q^2) i \varepsilon_{\mu\nu\rho\sigma} \varepsilon^\nu p^\rho p'^\sigma, \quad (14)$$

$$\langle \pi_8^a(p') | A^\mu | \omega_8^b(p) \rangle = \frac{\delta^{ab}}{\sqrt{m_{\pi_8} m_{\omega_8}}} \left[ A_1(q^2) m_{\pi_8} m_{\omega_8} \varepsilon^\mu + A_2(q^2) p' \cdot \varepsilon p^\mu + A_3(q^2) p' \cdot \varepsilon p'^\mu \right], \quad (15)$$

where  $p, p'$  are 4-momentum of  $\omega_8, \pi_8$  respectively,  $\varepsilon$  is the polarization vector of  $\omega_8$ , and  $V$  and  $A_{i=1,2,3}$  are form factors in  $q^2 \equiv (p - p')^2$

A straightforward calculation gives ( $\hat{m} \equiv m/m_{\omega_8}$ )

$$\Gamma(\omega_8 \rightarrow \pi_8 W) = \frac{G_F m_{\omega_8}^3}{32\sqrt{2}\pi} \frac{m_{\omega_8}}{m_{\pi_8}} W(\hat{m}_{\pi_8}, \hat{m}_W), \quad (16)$$

with

$$W(x, y) = |A_1|^2 x^2 (1 - 2x^2 + x^4 + 10y^2 - 2x^2 y^2 + y^4) \lambda + \text{Re}[A_1^*(A_2 + A_3)] x (1 - x^2 + y^2) \lambda^3 + \frac{1}{4} |A_2 + A_3|^2 \lambda^5 + 2|V^2| y^2 \lambda^3, \quad (17)$$

where  $\lambda = \lambda(1, x^2, y^2)$  as already defined. Here,  $M_W$  has to be kept, since transverse  $W$  emission has a  $\beta$  phase space factor, while longitudinal  $W$  emission has a  $\beta^3$  factor and more suppressed. Using the assumption that a free quark inside a meson interacts with currents, the form factors are reduced to  $V = -1$ ,  $2m_{\omega_8} m_{\pi_8} A_1 = (m_{\omega_8} + m_{\pi_8})^2 - q^2$ ,  $A_2 = -1$  and  $A_3 = 0$ . For simplicity, we use this limit in our numerical calculation, and Eq. (17) reduces to

$$W(x, y) \simeq (1 - 2x^2 + x^4 + 3y^2 + 2xy^2 + 3x^2 y^2 - 4y^4) \times (1 + 2x + x^2 - y^2) \lambda, \quad (18)$$

where  $\lambda = \lambda(1, x^2, y^2)$ .

A vector to vector transition amplitude via color octet vector current is parameterized as

$$\langle \omega_1(p') | V^{\mu,a} | \omega_8^b(p) \rangle = \frac{\delta^{ab}}{\sqrt{6}} \left[ (V_1(q^2) p^\mu + V_2(q^2) p'^\mu) \varepsilon' \cdot \varepsilon + V_3(q^2) p \cdot \varepsilon' \varepsilon^\mu + V_4(q^2) p' \cdot \varepsilon \varepsilon'^\mu \right], \quad (19)$$

where  $\varepsilon, \varepsilon'$  are the polarization vectors of  $\omega_8, \omega_1$ , respectively, and  $V_{i=1\dots 4}$  are form factors in  $q^2$ . A straightforward calculation gives ( $\hat{m} \equiv m/m_{\omega_8}$ )

$$\Gamma(\omega_8 \rightarrow \omega_1 g) = \frac{\alpha_s}{18} \frac{m_{\omega_8}^2}{m_{\omega_1}} G(\hat{m}_{\omega_1}), \quad (20)$$

where we take the scale of the strong coupling constant to be at the mass of  $\omega_8$ , and

$$G(x) = (1 - x^2)^3 \frac{|V_3|^2 + x^2 |V_4|^2}{2x^2}, \quad (21)$$

$$\simeq (1 - x^2)^3 / x. \quad (22)$$

The second step follows from taking the free-quark limit as described above, which reduces the form factors to  $V_1 = -V_3 = -\sqrt{m_{\omega_1}/m_{\omega_8}}$  and  $V_2 = -V_4 = -\sqrt{m_{\omega_8}/m_{\omega_1}}$ . We use this result, which is highly suppressed by phase space, for our numerical estimation.

### 4. Numerical estimates

To perform numerical studies of the branching ratios and decay widths, we finally have to specify the numerical values of the following parameters:  $\xi$ ,  $V_{t'b}$  ( $= -V_{tb'}$ ) and  $\Delta m = m_{\omega_8} - m_{\pi_8}$  for  $\omega_8 \rightarrow \pi_8 W$  ( $\Delta m = m_{\omega_8} - m_{\omega_1}$  for  $\omega_8 \rightarrow \omega_1 g$ ). Without a full solution to the relativistic

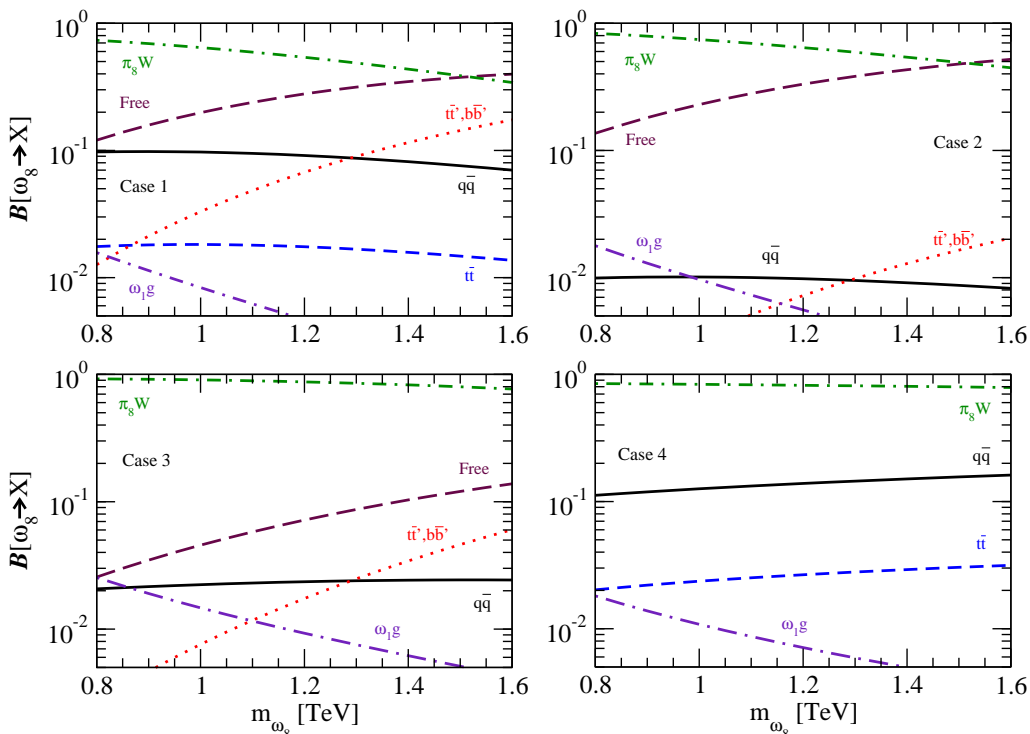


FIG. 7. Branching ratio of  $\omega_8$  as a function of  $m_{\omega_8}$  for given parameter sets in Case 1 to 4.

strong coupling bound state problem, however, it is difficult to ascertain the values for  $\xi = f_{\omega_8}/m_{\omega_8}$  as well as the mass splittings, and  $m_{\omega_8}$  itself. We therefore examine four sets of parameters as a survey,

- Case 1 :  $\xi = 0.1$ ,  $\Delta m = 100$  GeV,  $V_{t'b} = 0.1$ ;
- Case 2 :  $\xi = 0.03$ ,  $\Delta m = 100$  GeV,  $V_{t'b} = 0.1$ ;
- Case 3 :  $\xi = 0.1$ ,  $\Delta m = 200$  GeV,  $V_{t'b} = 0.1$ ;
- Case 4 :  $\xi = 0.1$ ,  $\Delta m = 100$  GeV,  $V_{t'b} = 0.01$ .

These are chosen simply to emphasize large variety of possible dominant decay channels. In all the cases we set the binding energy of  $\omega_8$  to  $m_{\omega_8} - 2m_Q = -100$  GeV, which is much larger than QCD binding. A different choice of the  $\omega_8$  binding energy changes our results only modestly. For the choices specified in Case 1, we assume the larger decay constant,  $\mathcal{O}(100)$  GeV mass difference in the meson spectrum, and  $V_{t'b}$  is set to the nominal current upper limit [7]. In Case 2, we examine the smaller decay constant. Case 3 is for larger mass difference, and Case 4 is when  $V_{t'b}$  is more suppressed. We will discuss the two different mass differences (vector–pseudoscalar and octet–singlet) as variations.

We plot in Fig. 7 the branching ratio of various  $\omega_8$  decays as a function of  $m_{\omega_8}$  for Cases 1 to 4. In Case 1, the dominant decay modes are the transition decay into  $\pi_8 W$ , especially for lighter mass region, and free quark decay, i.e. via the decay of 4G constituent quark for

heavier mass region. The branching ratios of free quark decay and the  $V_{t'b}$ -dependent annihilation ( $W$  boson exchange) decay increase with  $m_{\omega_8}$ , because  $m_{\omega_8} \sim 2m_Q$  reflects a larger Yukawa coupling. The  $q\bar{q}$  is of order 10% and drops slightly at higher  $m_{\omega_8}$ , with  $t\bar{t}$  branching ratio a factor of 5 lower, at the percent level. The transition decay into  $\omega_1 g$  is at the percent level or less.

In Case 2, because of the small decay constant, the annihilation decay channels  $t\bar{t}'$ ,  $b\bar{b}'$ ,  $q\bar{q}$  and  $t\bar{t}$  are suppressed. In this case, free quark decay and transition decay into  $\pi_8 W$  are the two predominant modes.

In Case 3, the large mass differences enhance the branching ratio of the transition decays, and the  $\pi_8 W$  mode dominates. The other transition decay into  $\omega_1 g$  can also be enhanced, especially in the lighter mass region. It could be that the mass difference of only  $m_{\omega_8} - m_{\omega_1}$  is large, i.e. when the mass spectrum is like  $m_{\omega_8} \simeq m_{\pi_8} > m_{\omega_1}$ . If so,  $\pi_8 W$  could be considerably suppressed, and  $\omega_1 g$  would be more prominent, especially for low  $m_{\omega_8}$ .

In Case 4, the free quark decay and the  $V_{t'b}$  induced annihilation decay are suppressed, due to small  $V_{t'b}$ . The decay width of 4G quarks is also suppressed for the same reason. In this case, the transition decay into  $\pi_8 W$  dominates, and the annihilation decay into dijets can be sub-dominant with branching ratio at ten percent order. However, this sensitively depends on the  $m_{\omega_8} - m_{\pi_8}$  mass difference, as well as the decay constant. If  $\pi_8 W$  becomes kinematically suppressed, dijets would be dominant.

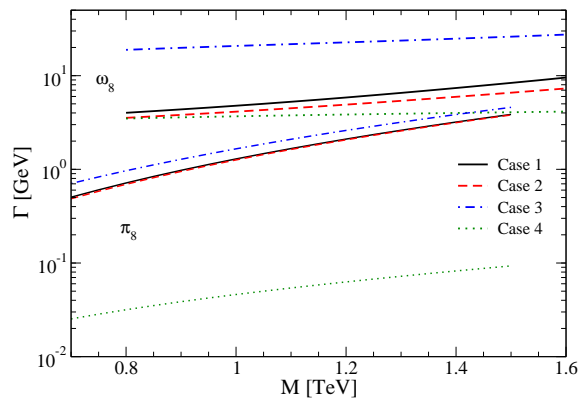


FIG. 8. Total decay width of  $\omega_8$  and  $\pi_8$  for the four parameter sets. The upper curves are for  $\omega_8$ , where Case 3 is enhanced by a larger  $m_{\omega_8} - m_{\pi_8}$  mass difference. The lower curves, plotted 100 GeV less in mass, are for  $\pi_8$ , where Cases 1 and 2 are barely distinguishable.

Let us summarize some general features regarding branching ratios. Basically, the transition decay into  $\pi_8 W$  is large, because of the large Yukawa coupling and no suppression effect by bound state deformation. This decay mode can be more enhanced if the mass difference is large, but much suppressed if the mass difference is small, especially if less than  $M_W$ , as we have seen. Free quark decay has sizable contribution for the heavier mass region, if  $V_{t'b}$  is close to the current upper limit of 0.1.

In Fig. 8, we show the total decay width of  $\omega_8$  as a function of  $m_{\omega_8}$  for the four parameter sets. The decay width increases with  $m_{\omega_8}$ , from a few GeV to around 10 GeV. For Case 3, due to the rapid decay into  $\pi_8 W$  from a relatively large  $m_{\omega_8} - m_{\pi_8}$  mass difference, the width is at 20 GeV range, and increases mildly with  $m_{\omega_8}$ . Still, compared with its TeV scale mass,  $\omega_8$  is a heavy but narrow meson resonance.

We see that the binding energy, therefore strong Yukawa dynamics, and flavor structure through  $V_{t'b}$  all play crucial role for the eventual phenomenology one expects at LHC.

### 5. The Decay of $\pi_8$

To be able to address LHC phenomenology, we need to treat  $\omega_1$  and  $\pi_8$  further, as they may appear in  $\omega_8$  decay final state. From Fig. 7 we see that in general  $\pi_8 W$  is the leading decay. Note, however, that we have assumed  $m_{\omega_8} - m_{\pi_8} = 100$  GeV. The rate would drop sharply as this vector–scalar splitting diminishes, and becomes practically negligible when  $W$  turns virtual. On the other hand, if the strong binding found by Ref. [16] in the Bethe–Salpeter approach with  $s$ -channel subtracted has any bearing, then  $\pi_8$  may be deeper bound than  $\omega_8$ . For this situation, Case 3 stands as an illustration, where  $\omega_8 \rightarrow \pi_8 W$  decay would be preminent.

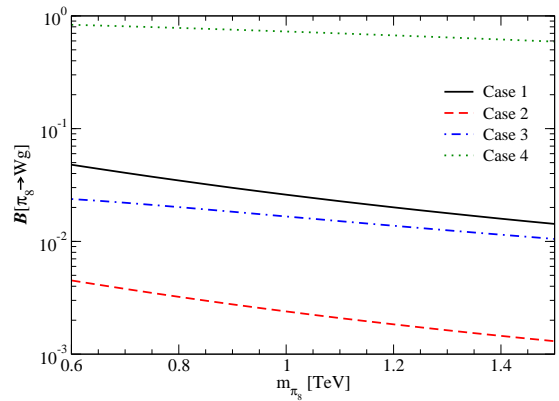


FIG. 9. Branching ratio  $\mathcal{B}(\pi_8 \rightarrow Wg)$  for the four parameter sets, ranging from predominance (Case 4), to below  $10^{-2}$  (Case 2).

In contrast, the process  $\omega_8 \rightarrow \omega_1 g$  is never more than 10%, and more typically at  $10^{-2}$  order or smaller. The exception would be if  $m_{\omega_8} - m_{\pi_8}$  is of order  $M_W$  or less, but  $m_{\omega_8} - m_{\omega_1}$  is sizable (plot of Case 3 in Fig. 7, but with  $\omega_8 \rightarrow \pi_8 W$  removed). Viewing this exception as unlikely, we relegate the discussion of  $\omega_1$  to a concurrent discussion of weak Drell–Yan production.

But we need to address how  $\pi_8$  decays. It is interesting that  $\pi_8 \rightarrow \pi_1 g$  vanishes because it is a  $0^- \rightarrow 0^-$  transition, which we have verified by direct computation. The  $W_L$  exchange diagram of Fig. 5(a) is absent for charged  $\pi_8^\pm$  (i.e.  $t'b'$  and  $b't'$  mesons) because of isospin, while the  $s$ -channel annihilation is absent by the octet/isovector nature. The upshot is that we are left with only two decay processes: the familiar free quark decay, and a new type of decay,  $\pi_8 \rightarrow Wg$ , where the  $W$  is transverse. The latter is an inverse process of  $\omega_8 \rightarrow \pi_8 W$ , with  $g$  replacing  $\omega_8$ . However, the annihilation rather than transition nature implies that  $\pi_8 \rightarrow Wg$  is relatively suppressed.

Direct computation gives

$$\Gamma(\pi_8 \rightarrow Wg) = 2\xi_\pi^2 \alpha_s \alpha_W m_{\pi_8} \frac{(1 - M_W^2/m_{\pi_8}^2)^3}{(1 + 4m_Q^2/m_{\pi_8}^2 - 2M_W^2/m_{\pi_8}^2)^2}, \quad (23)$$

where  $\xi_\pi = f_{\pi_8}/m_{\pi_8}$  is the  $\pi_8$  decay constant normalized by  $\pi_8$  mass. The rate of  $\pi_8 \rightarrow Wg$  is suppressed by  $\alpha_W/\alpha_s n_f$  compared to the rate of  $\omega_8 \rightarrow q\bar{q}$  of Eq. (5). We have checked explicitly that longitudinal  $W$  emission again vanishes.

We plot the  $\pi_8$  width in Fig. 8, and the  $\mathcal{B}(\pi_8 \rightarrow Wg)$  branching fraction, in Fig. 9. The width is at GeV order, narrower than  $\omega_8$ , but could be much smaller if a small  $V_{t'b}$  suppresses the free quark decay widths. Thus,  $\pi_8 \rightarrow Wg$  decay branching fraction is below 10%, and much smaller for Case 2 (suppressed by a smaller decay constant). For Case 4, the small  $V_{t'b}$  case,  $\pi_8 \rightarrow Wg$  could dominate.

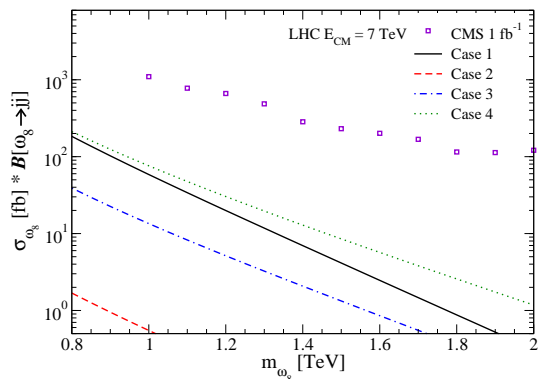


FIG. 10. Production cross section times branching ratio for  $\omega_8$  into dijets, for the four parameter sets at the LHC 7 TeV. CMS upper limit [31] for the cross section of dijet resonance production is also plotted.

#### IV. DISCUSSION

We now discuss the possible phenomenology, as well as other issues.

Let us first comment on the dijet decay of  $\omega_8$ , which could appear as a dijet resonance. Absence of dijet features in Tevatron and LHC searches constrains or rules out any model with particles in TeV range. In Fig. 10, we plot the total cross section times dijet branching ratio for  $\omega_8$  production at the LHC 7 running at TeV, as a function of  $m_{\omega_8}$  for the four parameter sets. We compare with the CMS dijet resonance search [31] with  $\mathcal{L} = 1 \text{ fb}^{-1}$  data at  $\sqrt{s} = 7 \text{ TeV}$ . We note that the data includes acceptance cuts for dijets, but our model numbers do not, which makes the comparison conservative. We find the cross section times dijet branching ratio are at least an order of magnitude lower than the current upper limit for all four Cases, with Case 4 the largest. Even with  $\omega_8 \rightarrow \pi_8 W$  channel removed making  $\omega_8 \rightarrow q\bar{q}$  the leading decay, one is still below the CMS limit. Let us call this special situation Case 4'. Our results show that, while a narrow resonance signal might start to show up with a considerably larger data set, it could show up soon for Case 4'. That is, if  $\omega_8 \rightarrow \pi_8 W$  decay is forbidden, while free quark and exchange decays are suppressed by small  $V_{t'b}$ . The need for these two conditions to be met, however, makes this possibility not particularly likely.

In general, the  $\omega_8 \rightarrow \pi_8 W$  decay is the dominant  $\omega_8$  decay mode, unless it is kinematically suppressed by  $m_{\omega_8} - m_{\pi_8}$  being too close to, or smaller than,  $M_W$ . We have investigated the decay of  $\pi_8$  itself, and found that it is dominated by free quark decay, with  $\pi_8 \rightarrow Wg$  subdominant for Cases 1–3. It is important now to spell out the isospin nature: isosinglet  $\omega_8^0 \rightarrow \pi_8^\pm W_s^\mp$ ,  $\pi_8^0 W_s^0$  with a 2 : 1 ratio, where the subscript  $s$  indicates a relatively soft vector boson, and  $W^0$  stands for the  $Z$  boson, as we have ignored heavy isospin breaking. Thus, the signature for  $q\bar{q} \rightarrow \omega_8 \rightarrow \pi_8 W$  leads to  $bW^+b'W_s^-$ ,  $tW^-t'W_s^+$ , and

$\{bW^+t', tW^-b'\}W_s^0$ , plus c.c. Except for the last case with presence of a  $Z$  boson (the identification via dileptons would be costly in branching fraction), the additional  $W^\pm$  which is relatively soft makes it an even more complicated signature than direct open  $Q\bar{Q}$  production. The same sign dilepton approach [29] remains a good one, but more jets would be present. Note that the  $Z$  is usually vetoed against in same sign dilepton studies.

However, if boosted  $W$  and top jets can be exploited to isolate the  $bW^+b'$  and  $tW^-t'$  (both in  $bWtW$  final state), then the associated soft  $W_s^\mp$  could be an extra tag for  $\pi_8^\pm W^\mp$  production. Besides the relatively low  $p_T$   $W$ , the 7-jet system has rich imbeddings of  $W$ ,  $b$  and  $t$  jets. It can be part of the  $t\bar{t}W$  search program, which would in any case be a background. But the multi-jet system is of rather high mass, and with different signature content, that one may be able to separate. If the total jet mass resolution is good, one may discover both the  $\pi_8^\pm$  in multijets with a soft  $W$  tag, with the  $\pi_8^\pm$  and the  $W^\mp$  reconstructing to  $\omega_8$ .

The LHC experiments should also look for a  $Z$  boson associated with high jet multiplicity, perhaps with a hint of unusual  $ZW$  plus multijets as backdrop. Given that  $\pi_8$  is very narrow, one could look for a relatively soft  $Z$  recoiling from 6 or 8 hadronic jets with very high, but relatively specific mass, containing substructures of multiple boosted  $W$  jets or boosted top jets. The whole event,  $Z + 6$  or 8 jets, would also reconstruct to a narrow resonant mass.

One might think that  $\gamma +$  multijets can be similarly pursued. However, Eq. (16) does not apply to  $\omega_8 \rightarrow \pi_8 \gamma$ : the  $V(q^2)$  term vanishes with  $M_W \rightarrow 0$ . The photonic decay involves heavy quark spin flip, hence suppressed by  $m_Q^2$ . Treating  $m_{\omega_8} + m_{\pi_8} \simeq 2m_{\omega_8}$ , since we allow  $\Delta m = m_{\omega_8} - m_{\pi_8} \sim 200 \text{ GeV}$  at best, the radiative rate is  $\Gamma(\omega_8 \rightarrow \pi_8 \gamma) \simeq \frac{\alpha}{3} \frac{(\Delta m)^3}{m_Q^2}$ . Since a larger  $\Delta m$  (Case 3) gives a larger total  $\omega_8$  width, we find that  $\mathcal{B}(\omega_8 \rightarrow \pi_8 \gamma)$  is always below the percent level. However, photon detection does not suffer from the factor of 0.06 as for  $Z \rightarrow \ell^+ \ell^-$  detection. Hence, the LHC experiments might also consider  $\gamma +$  multijet studies.

Case 4 offers yet again an intriguing signature, assuming  $\omega_8 \rightarrow \pi_8 W$  decay dominance. From Fig. 9 we see that  $\pi_8 \rightarrow Wg$  is dominant, as free quark decay is suppressed by a small  $V_{t'b}$ . One therefore has a unique signature of  $W_s Wg$  ( $W_s^\pm W^\mp g$  and  $Z_s Zg$ ). Here, one  $W$  is soft, and the other hard, with  $p_T$  greater than 500 GeV, accompanied by a similarly hard gluon. Both  $W$ 's tend to be transverse, but the hard  $W$ -jet and the gluon jet would form a rather narrow resonance! This case offers dramatic signature and should be quickly searched for. The production cross section, of course, is modulated by  $f_{\omega_8}$  (see Fig. 3). Case 4, which is the limiting case of small  $V_{t'b}$ , has better likelihood than the even more special Case 4' discussed earlier.

Leaving Case 4, i.e. if  $V_{t'b}$  is closer to 0.1, the next prominent decay compared with  $\omega_8 \rightarrow \pi_8 W$  in general is

“free” quark decay, i.e. one of the bound  $t'$  or  $b'$  quarks decays, dissolving the bound state system. This could be practically the only other decay mode, if the exchange and annihilation decays are suppressed by a small decay constant (Case 2). The signature is  $q\bar{q} \rightarrow \omega_8 \rightarrow bW\bar{t}'$ ,  $tW\bar{b}'$  (plus c.c.), where the notation implies the associated  $\bar{t}'$  or  $\bar{b}'$  decays on-shell, but the  $bW$  and  $tW$  are decay products of a bound, somewhat off-shell  $t'$  or  $b'$  quark, which is not too different from open  $Q\bar{Q}$  production. Unless the on-shell nature is used in the direct search, the search limits would not be affected. However, once 4G quarks are discovered, one should check whether, for some fraction of the events (depending on resonance vs open  $Q\bar{Q}$  production ratio), one of the heavy quarks is in fact off-shell, which would be an indication for bound state phenomena. We remark that open  $Q\bar{Q}$  production at the LHC is dominantly through  $gg$  fusion, while the  $\omega_8$  resonance production is through  $q\bar{q}$  fusion. There is little resonance phenomena in  $gg \rightarrow Q\bar{Q}$  via Yukawa effects. In fact, in the  $\eta_{(8)}$  channels, it is even repulsive. Thus, even above the unitarity bound, standard search can continue, except that there may be some “anomalies” as we have discussed, if any thing is found at all.

We have already dealt with the special case of dijet resonance for Case 4. Dijets from  $q\bar{q} \rightarrow \omega_8 \rightarrow q\bar{q}$  tend to be subdominant in all other Cases (i.e. 1–3), but it could be at 10% level. It would provide a spectacular dijet resonance signal, and definite measurement [32] of resonance mass, and spin if there is good signal over background. If the branching ratio could be measured in some way, one could access the important decay constant. In general, a resonance would also appear in  $t\bar{t}$  (boosted top jets), with cross section 1/5 the dijet resonance.

Finally, there is also the exchange decay to  $t\bar{t}'$  and  $b\bar{b}'$ , which is a subdominant channel typically below 10%. It mimics “single  $t'$  ( $b'$ )” production, and can be studied that way. But an associated boosted top, or a high  $p_T$   $b$ -jet that tags a resonant  $tW$ , could be quite distinct.

We offer some remarks on the  $A_{\text{FB}}^{t\bar{t}}$  [33] and  $Wjj$  [34] anomalies at the Tevatron. Naively, one might think that the presence of resonance production of  $t\bar{t}$  could be relevant for  $A_{\text{FB}}^{t\bar{t}}$ . But  $\omega_8$  has same quantum numbers as the gluon, i.e. the coupling to  $t\bar{t}$  is fully vector. Thus, it cannot generate  $A_{\text{FB}}^{t\bar{t}}$  suggested by Tevatron data. For the  $Wjj$  anomaly, the Yukawa bound resonances are so massive, they can have nothing to do with it.

This brings us to comparing with Technicolor (TC) models. Low scale TC has been invoked [35] for the  $Wjj$  anomaly suggested by CDF. Our  $\omega_8$  and  $\pi_8$  are Yukawa bound  $Q\bar{Q}$  mesons with an operative heavy isospin, from degenerate chiral quark doublet  $Q$  not too far above the unitarity bound. Thus, our  $\omega_8$  and  $\pi_8$  mesons are much heavier than those in low scale TC. For more generic TC models [36], since “walking” is generally required, the technipion  $\pi_T$  tends to be closer to the technirho  $\rho_T$  in mass such that  $\rho_T \rightarrow \pi_T\pi_T$  is absent, while (near) degeneracy of  $\omega_T$  and  $a_T$  with  $\rho_T$  is also often invoked. The signature for these technimesons are typically  $WZ$ ,  $W\gamma$

and  $Z\gamma$ . Thus, not only the spectrum is rather different — absence of  $\rho$  and  $a$  mesons — the decay signature is also in strong contrast. The bound states due to strong Yukawa coupling, which follow simply from the existence of new heavy chiral quarks without assuming new dynamics, should be easily distinguished from Technicolor.

The Yukawa-bound ultraheavy mesons are also quite distinct from QCD bound states. Not only there is the absence of  $\eta$  (where  $gg$  fusion would be possible) and  $\rho$  type mesons, they have a much larger binding energy, and are much smaller in size. This is brought about by not only a strong coupling constant, but facilitated by a  $\gamma_5$  coupling due to Goldstone or longitudinal vector bosons; the  $0^+$  Higgs boson, being heavy, would in fact be subdominant. Thus, the tight bound states involve ultrarelativistic motion of its very heavy constituents, hence somewhat counterintuitive. By far we have not attempted any actual solution of the bound state problem here. We therefore chose to remain close to the unitarity bound, considering bound state masses not more than 1.5 TeV. We have chose to parameterize with a few key parameters. Our numerics, and associated phenomenology, should be viewed as only illustrative, with the *key parameters to be determined by experiment*.

What mass scale would Nature actually choose, if she so chooses to offer an extra chiral doublet above the existing three generations? It may be related to the electroweak symmetry breaking through  $\bar{Q}Q$  condensation. It could in principle lead to very deeply bound states, with binding energy approaching  $m_Q$  order or more. We have only scratched the surface of Yukawa-bound heavy mesons, the treatment of which would require genuine nonperturbative methods, such as [12] lattice field theory. Paradoxically, it is not impossible that heavier quark masses than considered here could result in lower heavy meson masses. Again, experiment might take the lead here.

## V. CONCLUSION AND OUTLOOK

With the experimental limits on sequential chiral 4th generation already at 500 GeV, i.e. at the doorsteps of the unitarity bound, we have considered the possibility of new  $Q\bar{Q}$  mesons bound by strong Yukawa couplings. Comparing a relativistic expansion approach (which indicated nonapplicability), versus a relativistic Bethe–Salpeter equation approach, we chose to illustrate what might appear in early data of LHC running, i.e. bound states just above the TeV scale, but with relatively complicated decay final states.

Electroweak precision tests suggest a new (heavy) isospin symmetry, such that the leading production would be a color octet, isosinglet vector meson, which we call  $\omega_8$ . It can be produced via  $q\bar{q} \rightarrow \omega_8$  fusion, through an unknown decay constant,  $f_{\omega_8}$ . For decay, the key parameters besides  $f_{\omega_8}$  are the quark mixing element  $V_{t'b}$ , and the mass differences  $m_{\omega_8} - m_{\pi_8}$  and  $m_{\omega_8} - m_{\omega_1}$

where  $\pi_8$  is a heavy color octet “pion” and  $\omega_1$  a color singlet “omega”. We find the leading decay is likely  $\omega_8 \rightarrow \pi_8 W$ , while the other transition channel into  $\omega_1 g$  is relatively suppressed. The other leading decay is “free”, or constituent, quark decay. Illustrating with four Cases for large/small decay constant, nominal/suppressed mass differences or  $V_{t'b}$ , together with the two decay channels of free quark decay and  $Wg$  decay of  $\pi_8$ , we considered the possible LHC phenomenology. We find in general the  $\omega_8$  to be narrow compared to its mass.

The special case of small  $V_{t'b}$  leads to two possible spectacular signatures. One is  $q\bar{q} \rightarrow \omega_8 \rightarrow \pi_8 W_s \rightarrow W_s Wg$ , where a massive back-to-back  $Wg$  system is accompanied by a relatively soft  $W$ . This mode could become suppressed if  $m_{\omega_8} - m_{\pi_8}$  is close to or less than  $M_W$ . Then, one could have a dijet resonance close to current LHC limits, and a narrow dijet resonance could appear soon. In the general case, dijet signal is suppressed by a decay branching ratio.

Other than the above two (perhaps unlikely) spectacular signals, the generic leading decay is  $\omega_8 \rightarrow \pi_8^\pm W_s^\mp$ ,  $\pi_8^0 Z_s^0$ , followed by free quark decay of  $\pi_8$  ( $\pi_8 \rightarrow Wg$  is typically subdominant). This leads to possible multijet signals with an associated relatively soft  $W$  or  $Z$  tag, where the multijet system is very massive, and with multiple  $b$ ,  $W$  and  $t$  jet substructures. If such massive multijet systems can be studied, one could possibly reconstruct both the  $\pi_8$  and  $\omega_8$  resonances. Assuming single channel dominance, one can measure the meson decay constant

by the total cross section.

If  $\omega_8 \rightarrow \pi_8 W$  is suppressed by kinematics, however, the likely leading decay would be by the constituent heavy quark decay, which is very similar to standard  $Q\bar{Q}$  signal, except one heavy quark decays somewhat off-shell. Since in any case the leading  $gg \rightarrow Q\bar{Q}$  fusion does not exhibit resonance phenomena, *the current 4th generation  $t'\bar{t}'$  and  $b'\bar{b}'$  search can continue beyond the unitarity bound*. But if 4G quarks are discovered, then some good fraction of the events would have one quark decaying below threshold, indicating bound state phenomena. One, of course, would have to disentangle also  $\omega_8 \rightarrow \pi_8 W$ , as already discussed.

We have provide some definite signatures for Yukawa-bound heavy  $Q\bar{Q}$  mesons in the 1 to 1.5 TeV range. But our study is only of precursory nature. As LHC energy increases, and with higher luminosity, it could uncover new chiral quarks above the unitarity bound, with new unusual bound states. One could probe into the truly nonperturbative regime, which our results only offer a glimpse of what might happen. There may be a host of new heavy mesons awaiting us beyond the horizon.

**Acknowledgement.** We thank K.-F. Chen, A. Djouadi, K. Ishiwata, B. Kniel, T. Kugo, M.B. Wise, B.-L. Young and C.-P. Yuan for discussions, and K. Hagiwara for encouraging comments. WSH thanks the National Science Council for Academic Summit grant NSC 99-2745-M-002-002-ASP, and TE and HY are supported under NSC 100-2811-M-002-061 and NSC 100-2119-M-002-001.

- 
- [1] Plenary talk by G. Tonelli at Europhysics Conference on High-Energy Physics, July 2011, Grenoble, France.
  - [2] Plenary talk by A. Nisati at Lepton Photon Symposium, August 2011, Mumbai, India.
  - [3] Plenary talk by A. De Roeck at Lepton Photon Symposium, August 2011, Mumbai, India.
  - [4] M.S. Chanowitz, M.A. Furman and I. Hinchliffe, Phys. Lett. B **78**, 285 (1978); Nucl. Phys. B **153**, 402 (1979).
  - [5] This has been explored, in the context of the Nambu–Jona-Lasinio model, by W.A. Bardeen, C.T. Hill and M. Lindner, Phys. Rev. D **41**, 1647 (1990). The authors credit the idea to Y. Nambu, “Bootstrap Symmetry Breaking in Electroweak Unification”, EFI preprint 89-08 (1989).
  - [6] B. Holdom, Phys. Rev. Lett. **57**, 2496 (1986).
  - [7] For a recent brief review on the 4th generation, see B. Holdom *et al.*, PMC Phys. A **3**, 4 (2009).
  - [8] B.W. Lee, C. Quigg and H.B. Thacker, Phys. Rev. Lett. **38**, 883 (1977); Phys. Rev. D **16**, 1519 (1977).
  - [9] Plenary talk by A. Djouadi at Lepton Photon Symposium, August 2011, Mumbai, India.
  - [10] K. Nakamura *et al.* [Particle Data Group], J. Phys. G **37**, 075021 (2010).
  - [11] W.-S. Hou, Chin. J. Phys. **47**, 134 (2009) [arXiv:0803.1234 [hep-ph]].
  - [12] Talk by C.-J.D. Lin at Lattice 2011 Conference, July 2011, Squaw Valley, California, USA.
  - [13] M. E. Peskin, T. Takeuchi, Phys. Rev. Lett. **65**, 964-967 (1990); Phys. Rev. **D46**, 381-409 (1992).
  - [14] G.D. Kribs, T. Plehn, M. Spannowsky and T.M.P. Tait, Phys. Rev. D **76**, 075016 (2007); H.-J. He, N. Polonsky and S.-f. Su, Phys. Rev. D **64**, 053004 (2001); V.A. Novikov, L.B. Okun, A.N. Rozanov and M.I. Vysotsky, JETP Lett. **76**, 127 (2002) [Pisma Zh. Eksp. Teor. Fiz. **76**, 158 (2002)].
  - [15] K. Ishiwata and M.B. Wise, Phys. Rev. D **83**, 074015 (2011).
  - [16] P. Jain *et al.*, Phys. Rev. D **46**, 4029 (1992); *ibid.* D **49**, 2514 (1994).
  - [17] Dynamical arguments give a much higher bound on the 4G fermion masses at several TeV. See e.g. M.B. Einhorn and G.J. Goldberg, Phys. Rev. Lett. **57**, 2115 (1986).
  - [18] See, for example, H. Inazawa and T. Morii, Phys. Lett. B **203**, 279 (1988) [Erratum-*ibid.* B **207**, 520 (1988)].
  - [19] A form of “ $\pi_8$ ”, or color octet isovector pseudoscalar, meson pair production has been considered by B.A. Dobrescu and G.Z. Krnjaic, arXiv:1104.2893 [hep-ph].
  - [20] E. Arik, O. Cakir, S.A. Cetin and S. Sultansoy, Phys. Rev. D **66**, 116006 (2002).
  - [21] For a general discussion, see for example, T. Kugo, Phys. Lett. B **76**, 625 (1978).
  - [22] J. Pumplin *et al.*, JHEP **0207**, 012 (2002).
  - [23] R. Baier and R. Rückl, Z. Phys. C **19**, 251 (1983).
  - [24] V.D. Barger *et al.*, Phys. Rev. D **35**, 3366 (1987)

- [Erratum-*ibid.* D **38**, 1632 (1988)].
- [25] P. Nason, S. Dawson and R.K. Ellis, Nucl. Phys. B **303**, 607 (1988).
- [26] A. Petrelli *et al.*, Nucl. Phys. B **514**, 245 (1998).
- [27] Y. Sumino *et al.*, Phys. Rev. D **47**, 56 (1993).
- [28] M. Jezabek, J.H. Kühn and T. Teubner, Z. Phys. C **56**, 653 (1992).
- [29] S. Chatrchyan *et al.* [CMS Collaboration], Phys. Lett. B **701**, 204 (2011).
- [30] This effect is examined for the top quark case in the  $t\bar{t}$  resonance region, in Y. Sumino and H. Yokoya, JHEP **1009**, 034 (2010).
- [31] S. Chatrchyan *et al.* [CMS Collaboration], arXiv:1107.4771 [hep-ex].
- [32] Y. Kats and M.D. Schwartz, JHEP **1004**, 016 (2010).
- [33] T. Aaltonen *et al.* [CDF Collaboration], Phys. Rev. D **83**, 112003 (2011); V.M. Abazov *et al.* [D0 Collaboration], arXiv:1107.4995 [hep-ex].
- [34] T. Aaltonen *et al.* [CDF Collaboration], Phys. Rev. Lett. **106**, 171801 (2011). Note that this has been refuted by the D0 Collaboration, V.M. Abazov *et al.* [D0 Collaboration], *ibid.* **107**, 011804 (2011).
- [35] E.J. Eichten, K. Lane and A. Martin, Phys. Rev. Lett. **106**, 251803 (2011).
- [36] See A. Martin, arXiv:0812.1841 [hep-ph], for a brief review.